THE ASTRONOMICAL JOURNAL VOLUME 78, NUMBER 1 FEBRUARY 1973

Asteroid spectral reflectivities*†

Clark R. Chapman‡, Thomas B. McCord, and Torrence V. Johnson§

Planetary Astronomy Laboratory, Department of Earth and Planetary Sciences, Massachusetts Institute of Technology, Cambridge, Massachusetts 02139

(Received 20 September 1972; revised 27 October 1972)

We measured spectral reflectivities (0.3–1.1 μm) for 32 asteroids. There are at least 14 different curve types. Common types are: (a) reddish curves with 10% absorptions near 0.95 μm or beyond 1.0 μm, due to Fe^{2+} in minerals such as pyroxenes; (b) flat curves in the visible and near-IR with sharp decreases in the UV and (c) flat curves even into the UV. Several asteroids show probable color variations with rotation, especially 6 Hebe. A sample of 102 asteroids with reliably known colors is derived from the reflectivities and from earlier colorimetry. Several correlations of colors and spectral curve types with orbital and physical parameters are examined: (1) Asteriods with large aphelia have flat reflectivities while those with small perihelia are mostly reddish. (2) Curve types show evidence for clustering on an *a* vs *e* plot, with 0.95 μm bands occuring mainly for Mars-approaching asteroids. (3) No strong correlation exists between color and either proper eccentricity or proper inclination. (4) The Flora group asteroids are reddish, but most families have members of different colors; hence most families are not composed of fragments of homogeneous bodies. (5) Color is not correlated with rotation period, but is weakly correlated with lightcurve amplitude. (6) Color seems strongly correlated with asteroid diameter; no large asteroids are reddish, no small ones have flat reflectivities.

INTRODUCTION

ASTEROID spectral reflectivities are useful in two ways. First, the slopes, absorption band positions, and other characteristics of reflectivity curves are diagnostic of mineralogy, particle size, and other properties of asteroid surfaces. Second, they allow recognition of differences between asteroids which may be correlated with other characteristics, such as orbital parameters.

Several dozen asteroids have accurately measured *UBV* colors (Gehrels 1970; Taylor 1971) but only one asteroid has had its visible and near-IR reflectivity spectrum accurately determined (McCord *et al.* 1970). Now we have determined curves for 31 additional asteroids. In this paper we describe the observational program, present the reflectivities, and discuss the correlation of asteroid colors (as determined from both this program and earlier colorimetry) with other asteroidal parameters. A companion paper (Chapman 1972) will consider the implied mineralogies and textures of asteroid surfaces, and will relate these results to meteorites and the origin of the asteroids. A preliminary description of the program described here was presented by Chapman *et al.* (1971). More detailed descriptions of observing techniques, reduction procedures, and the analysis, as well as presentation of all the data, may be found in Chapman's (1971) doctoral dissertation, from which the present paper has been abstracted and updated.

I. SPECTRAL REFLECTIVITY OBSERVATIONAL PROGRAM

Asteroids were observed during the period June 1970 to May 1971 using a double-beam photometer (McCord 1968). A high-speed, computer-controlled pulse-counting data system was used for recording and monitoring the data in the two channels (object and sky, 40 msec samples). Dark current, scattered light, and differences in the double-beam mirror reflectivities were monitored and were recorded, along with the asteroid data, on magnetic tape. The photometer was operated in both double-beam and single-beam modes, using the set of 24 narrow-band interference filters described in Table I, to cover the spectral range 0.3 to 1.1 μm. S-1 and S-20 dry-ice-cooled ITT photomultipliers were used as detectors. Complete runs through the 24 filters took from between several minutes for bright objects, when the filter wheel was spun at 3 rpm and the signal co-added, to about an hour for faint asteroids when an incremental filter mode was used. [Asteroid rotation was not a problem, except possibly for 43 Ariadne which showed discordant colors (see Sec. III).] Asteroids were selected from among the available sample brighter than apparent magnitude 13.0; those chosen have both typical and extreme values of many physical and orbital parameters. There were seven observing runs on the 200-inch telescope at Mt. Palomar, 24- and 60-inch reflectors at Mt. Wilson, and the 36-inch reflector (No. 2) at Kitt Peak National Observatory.

The data are believed to be generally free from error at the 3% to 5% level. Some runs suffered from low signal-to-noise ratio, guiding and seeing problems, and difficulties in calibrating neutral density filters used for some standard star observations. Such runs have been given low or zero weight in obtaining the average reflectivity curves presented in this paper. Accuracy is always better in visible wavelengths than in the UV or IR because of higher count rate and more constant atmospheric conditions. The data show high internal consistency and are reproducible from night to night under different conditions.

II. DATA REDUCTION

Forty-eight numbers were obtained from each run on an asteroid or standard star: the brightness of both

object and sky in each of the 24 filters. Tests for beam mirror inequality, asymmetric scattered light, and other potential problems rarely showed effects large enough to require correction. Corrections were applied to some S-20 standard star observations to account for the neutral-density filter function and for nonlinearity in the data-system response to the signal at high count rates. A computer program was written to estimate temporal and spatial variations in the extinction coefficient and to correct for air mass differences between asteroids and standard stars.

The spectral reflectivity of an asteroid illuminated by the Sun was obtained from the formula

$$R_{\text{ast}} \propto \frac{\text{asteroid}}{\text{Sun}} = \left(\frac{\text{asteroid}_{\text{ob}}}{\text{star}_{\text{ob}}}\right)\left(\frac{\text{star}}{\text{Vega}}\right)\left(\frac{\text{Vega}}{\text{Sun}}\right), \quad (1)$$

where the quantities are fluxes integrated across the effective spectral response of each filter. For purposes of comparison and because there is no reliable information on asteroid albedos, the reflectivities were scaled to unity at 0.57 μm (usually the unsmoothed value of the 11th filter). The relative fluxes of the standard stars from Oke (1964) and Hayes (1970) were interpolated from the calibrations against Alpha Lyrae (Vega) at the effective wavelengths of each filter, taking due account of the spectral responses of the atmosphere, mirrors, and photocathodes. The stellar spectra were related to that of the Sun using a model for Alpha Lyrae (Schild *et al.* 1971) which takes lines into account and agrees well with observational absolute calibrations of the star (Oke and Schild 1970). The new solar spectrum of Arvesen *et al.* (1969) was adopted, which again takes account of lines in the solar spectrum. These new calibrations were updated from those used previously by the Planetary Astronomy Laboratory (see Appendix).

The calibration errors are believed to be dominated by the uncertainties in the relative calibrations between stars and Alpha Lyrae. These errors (mostly scatter but some systematic component) are about 2% in the visible, but are larger in the UV and may approach 4% in the IR in some cases. Such errors may significantly affect measurements of centers of mineral absorption bands. These calibration errors are probably larger than any other systematic errors in the data and are much larger than random scatter for the brighter asteroids.

III. SPECTRAL REFLECTIVITIES OF 32 ASTEROIDS

Reflectivities for the 31 asteroids, plus 4 Vesta (observed by T. Johnson and J. Kunin; Chapman *et al.* 1971), are presented in Fig. 1 and Table II. They are the averages of all runs made on each asteroid. Differences between asteroids may be compared more reliably than their absolute characteristics. Calibration of the first filter (0.3 μm) is worthless, while that for the fifth filter (0.38 μm) is subject to 5% to 10% errors due to the Balmer jump; data for both filters are omitted from Fig. 1.

TABLE I. Interference filters.

No.	Wavelength (μm)	Bandpass (μm)	Peak transmission	$\lambda_{\text{eff}}^{\text{S-20}}$	$\lambda_{\text{eff}}^{\text{S-1}}$
1[a]	0.3010	0.019	0.13	...	0.3100 ?
2	0.3196	0.016	0.19	0.3216	0.3229
3	0.3383	0.022	0.14	0.3406	0.3412
4	0.3590	0.014	0.18	0.3598	0.3593
5[b]	0.3831	0.013	0.23	0.3833	0.3825
6	0.4019	0.028	0.48	0.4021	0.4015
7	0.4344	0.028	0.42	0.4344	0.4340
8	0.4687	0.033	0.49	0.4684	0.4685
9	0.5001	0.029	0.57	0.4998	0.5001
10	0.5336	0.033	0.46	0.5331	0.5336
11[c]	0.5662	0.029	0.55	0.5658	0.5663
12	0.5993	0.032	0.54	0.5987	0.5994
13	0.6328	0.032	0.56	0.6322	0.6326
14	0.6649	0.027	0.50	0.6645	0.6649
15	0.6991	0.026	0.54	0.6986	0.6992
16	0.7299	0.033	0.51	0.7287	0.7300
17	0.7640	0.031	0.57	0.7628	0.7640
18	0.8078	0.049	0.46	0.8016	0.8072
19	0.8551	0.047	0.48	0.8499	0.8551
20	0.9063	0.048	0.58	...	0.9058
21	0.9475	0.051	0.59	...	0.9469
22	1.0036	0.050	0.53	...	1.0025
23	1.0548	0.050	0.55	...	1.0525
24	1.1033	0.049	0.44	...	1.1009

[a] Filter 1: destroyed, November 1970.
[b] Filter 5: data poor due to Balmer discontinuity in standard stars.
[c] Filter 11: normalizing filter.

There are some calibration problems for observations made with the S-20 photomultiplier. Particularly uncertain is the absolute calibration between the S-1 IR segment and the S-20 UV-visible segment for asteroids 12, 51, and 93. The averaging of S-20 runs (filters 1–18) with S-1 runs (all filters) made at different phases or rotational phases occasionally yields spurious effects near the 0.85 μm S-20 cutoff; the strongest such effect is a spurious enhancement of the 0.9 μm band for 6 Hebe.

Reflectivities may not be representative of all sides of an asteroid (evidence for rotational variations is given below). No color corrections for phase angle changes are applied, for reasons also discussed below. Two separate runs on 43 Ariadne on one night are badly discordant in over-all slope, which may be real; the reflectivity average presented is calculated using one of the two runs which agrees closely with a high-quality run made on another night.

IV. DESCRIPTION OF SPECTRAL REFLECTIVITY CURVES

The 32 asteroids observed so far show a variety of spectral reflectivity curves. That asteroids differ in color has been known since Bobrovnikoff's (1929) early result. But the extent of variety is evidently even greater than revealed in plots of B-V vs U-B; some asteroids with identical UBV colors differ noticeably

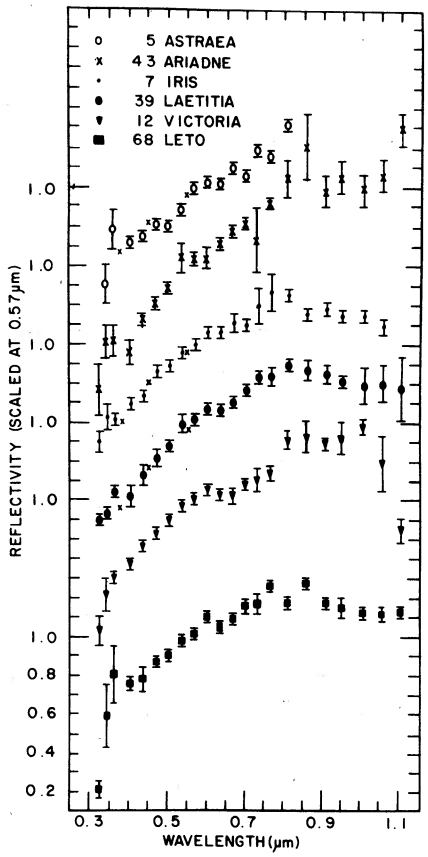

(a)

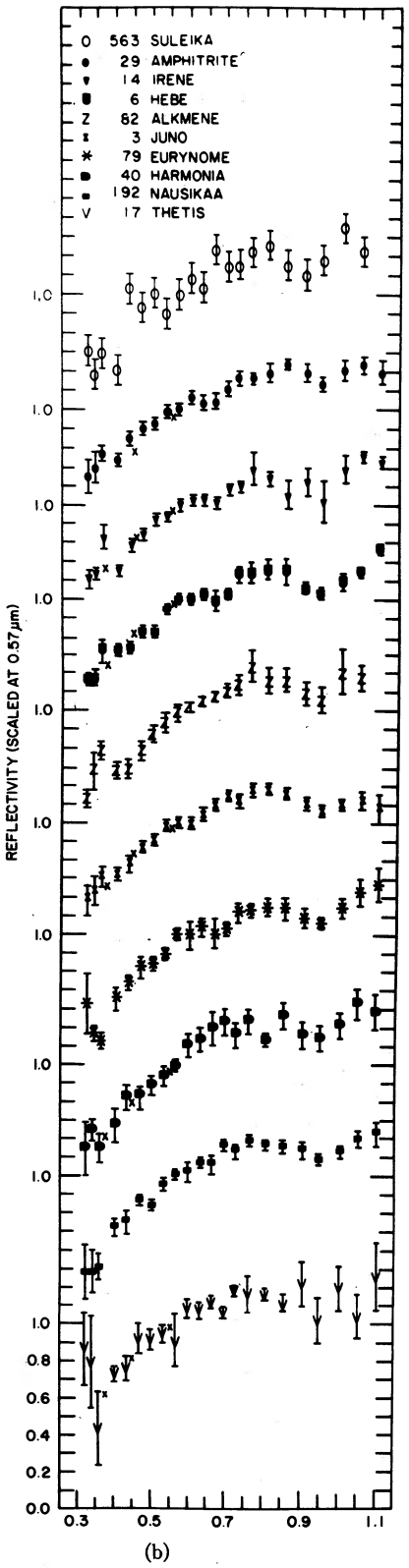

(b)

FIG. 1. Spectral reflectivity curves for 32 asteroids, scaled to unity (1.0) at 0.57 μm. Although all reflectivities are plotted to the same vertical scale, shown near the bottom of the vertical axis, they are vertically separated from each other for clarity. Small *x*'s indicate approximate conversions of Gehrels' (1970) *UBV* colors for some asteroids (see text).

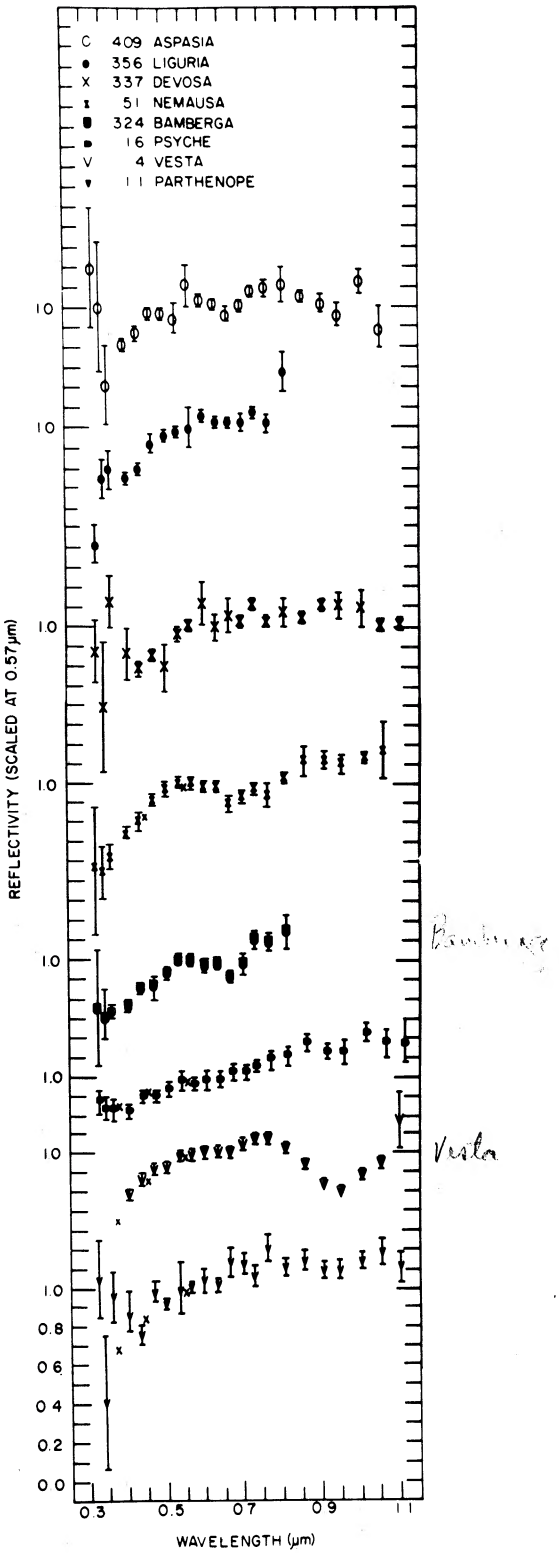

(c)

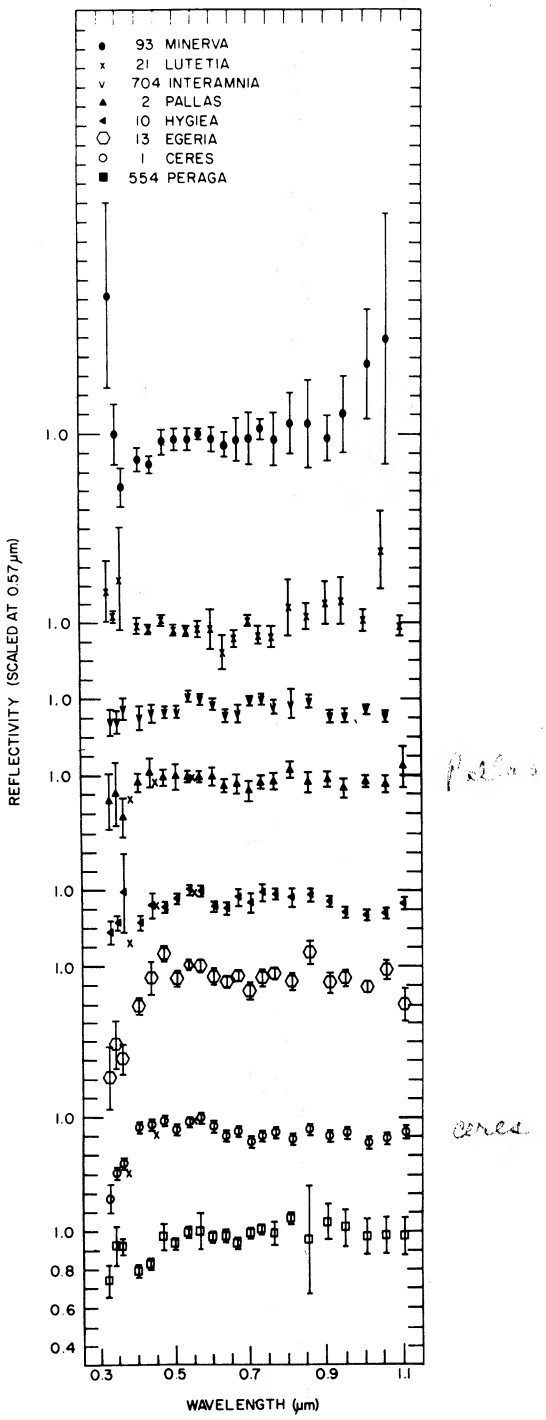

(d)

FIG. 1 (a)–(d) (*continued*)

TABLE II. Asteroid spectral reflectivities.

Wavelength μm	Asteroid Number										
	1	2	3	4	5	6	7	10	11	12	13
0.301	0.90	1.17	...	...	...	...	...	...	1.06	...	1.10
0.322	0.57	0.87	0.58	...	1.17	0.56	0.50	0.78	1.04	0.32	0.41
0.341	0.70	0.91	0.63	...	0.51	0.60	0.63	0.83	0.41	0.51	0.58
0.360	0.76	0.78	0.71	...	0.79	0.70	0.62	0.99	0.95	0.60	0.50
0.383	0.91	1.05	0.70	...	0.52	0.72	0.60	0.85	0.71	0.58	0.90
0.402	0.95	0.97	0.72	0.79	0.72	0.72	0.70	0.84	0.88	0.67	0.78
0.434	0.96	1.02	0.78	0.87	0.75	0.73	0.74	0.92	0.76	0.76	0.94
0.468	0.98	1.00	0.87	0.92	0.81	0.82	0.86	0.92	0.98	0.83	1.07
0.500	0.94	1.00	0.91	0.93	0.81	0.83	0.89	0.96	0.91	0.89	0.93
0.533	0.98	1.00	0.99	0.99	0.89	0.95	0.96	1.01	0.97	0.96	1.01
0.566	1.00	1.00	1.00	1.00	1.00	1.00	1.00	1.00	1.00	1.00	1.00
0.599	0.95	1.00	1.00	1.01	1.03	1.00	1.06	0.92	1.03	1.05	0.94
0.632	0.90	0.95	1.05	1.01	1.03	1.02	1.06	0.91	1.02	1.02	0.91
0.665	0.93	0.96	1.10	1.00	1.10	0.99	1.11	0.97	1.14	1.02	0.94
0.699	0.87	0.92	1.15	1.05	1.07	1.03	1.10	0.94	1.12	1.08	0.87
0.729	0.90	0.97	1.12	1.08	1.19	1.13	1.19	0.99	1.06	1.10	0.94
0.763	0.92	0.97	1.18	1.07	1.16	1.14	1.27	0.98	1.21	1.13	0.96
0.807	0.89	1.04	1.19	1.02	1.32	1.16	1.25	0.97	1.11	1.31	0.92
0.855	0.94	0.97	1.17	0.94	0.95	1.15	1.16	0.98	1.14	1.32	1.07
0.906	0.90	0.99	1.11	0.83	...	1.07	1.18	0.95	1.09	1.29	0.91
0.947	0.92	0.94	1.07	0.79	...	1.04	1.15	0.88	1.09	1.32	0.93
1.003	0.87	0.98	1.11	0.88	...	1.10	1.15	0.87	1.14	1.38	0.89
1.053	0.89	0.96	1.13	0.94	...	1.15	1.09	0.88	1.18	1.19	0.98
1.101	0.93	1.05	1.09	1.16	...	1.27	...	0.93	1.11	0.84	0.80

Wavelength μm	Asteroid Number										
	14	16	17	21	29	39	40	43	51	68	79
0.301	...	1.75	0.40	...	0.76	...	2.69	...	...	...	1.85
0.322	0.60	0.87	0.87	1.17	0.65	0.50	0.55	0.36	0.55	0.21	0.62
0.341	0.63	0.83	0.79	1.03	0.70	0.53	0.64	0.61	0.54	0.58	0.47
0.360	0.83	0.83	0.43	1.23	0.77	0.65	0.55	0.62	0.62	0.80	0.43
0.383	0.70	0.81	0.87	1.01	0.67	0.58	0.84	0.56	0.60	0.69	0.58
0.402	0.65	0.82	0.73	0.99	0.74	0.62	0.67	0.56	0.75	0.75	0.65
0.434	0.79	0.90	0.76	0.96	0.85	0.73	0.82	0.72	0.80	0.77	0.73
0.468	0.84	0.91	0.92	1.01	0.90	0.82	0.82	0.81	0.91	0.86	0.81
0.500	0.92	0.95	0.91	0.96	0.93	0.88	0.89	0.88	0.97	0.89	0.84
0.533	0.94	0.99	0.94	0.96	0.99	1.00	0.94	1.04	1.00	0.97	0.89
0.566	1.00	0.98	0.91	0.96	1.00	1.02	1.00	1.04	1.00	1.01	1.00
0.599	1.03	1.00	1.08	0.97	1.06	1.07	1.11	1.04	0.98	1.10	0.99
0.632	1.03	1.00	1.07	0.84	1.04	1.07	1.14	1.11	0.98	1.04	1.03
0.665	1.01	1.03	1.12	0.91	1.04	1.11	1.20	1.18	0.89	1.09	1.00
0.699	1.08	1.04	1.06	1.01	1.11	1.17	1.23	1.22	0.93	1.15	1.03
0.729	1.10	1.07	1.18	0.93	1.16	1.24	1.16	1.13	0.98	1.16	1.12
0.763	1.19	1.09	1.16	0.92	1.16	1.24	1.23	1.32	0.94	1.25	1.13
0.807	1.14	1.12	1.16	1.08	1.19	1.30	1.14	1.44	1.03	1.17	1.15
0.855	1.05	1.19	1.11	1.03	1.23	1.27	1.27	1.61	1.12	1.27	1.14
0.906	1.12	1.14	1.21	1.11	1.19	1.25	1.16	1.38	1.13	1.17	1.09
0.947	1.02	1.14	1.02	1.12	1.13	1.21	1.14	1.45	1.10	1.14	1.06
1.003	1.19	1.24	1.19	1.01	1.21	1.20	1.22	1.39	1.13	1.11	1.15
1.053	1.25	1.18	1.04	1.37	1.23	1.21	1.33	1.46	1.18	1.11	1.23
1.101	1.23	1.20	1.26	0.97	1.19	1.18	1.29	1.69	...	1.12	1.28

TABLE II (*continued*)

Wavelength μm	Asteroid Number									
	82	93	192	324	337	356	409	554	563	704
0.301	...	...	1'.28	...	...	...	...	...	...	...
0.322	0.53	1.72	0.48	0.75	0.87	0.40	1.20	0.74	0.71	0.88
0.341	0.68	1.00	0.48	0.72	0.58	0.74	1.00	0.92	0.58	0.88
0.360	0.78	0.72	0.51	0.74	1.12	0.79	0.61	0.91	0.69	0.95
0.383	0.58	0.55	0.57	0.88	0.60	0.45	0.72	0.75	0.67	0.84
0.402	0.68	0.87	0.72	0.76	0.86	0.75	0.81	0.79	0.60	0.90
0.434	0.69	0.84	0.75	0.85	0.78	0.79	0.87	0.83	1.03	0.93
0.468	0.79	0.96	0.87	0.86	0.85	0.92	0.97	0.97	0.93	0.93
0.500	0.88	0.97	0.84	0.93	0.79	0.96	0.96	0.93	1.01	0.93
0.533	0.94	0.98	0.95	1.01	0.96	0.98	0.95	0.99	0.90	1.02
0.566	0.99	1.00	1.01	1.00	1.00	1.00	1.11	1.00	1.00	1.00
0.599	1.02	0.97	1.02	0.97	1.11	1.06	1.03	0.97	1.09	0.97
0.632	1.05	0.95	1.07	0.98	0.99	1.03	1.01	0.98	1.04	0.91
0.665	1.08	0.97	1.06	0.91	1.05	1.02	0.96	0.94	1.23	0.92
0.699	1.11	0.98	1.16	0.98	1.02	1.02	1.00	0.99	1.15	0.99
0.729	1.14	1.03	1.12	1.10	1.11	1.07	1.08	1.01	1.16	1.00
0.763	1.24	0.97	1.19	1.10	1.02	1.02	1.09	0.99	1.22	0.96
0.807	1.16	1.06	1.17	1.14	1.07	1.28	1.11	1.07	1.26	0.97
0.855	1.17	1.05	1.16	...	1.04	...	1.05	0.96	1.16	0.99
0.906	1.10	0.98	1.14	...	1.11	...	1.02	1.05	1.10	0.91
0.947	1.07	1.11	1.09	...	1.10	...	0.96	1.02	1.18	0.91
1.003	1.21	1.37	1.12	...	1.09	...	1.12	0.98	1.35	0.94
1.053	1.17	1.50	1.20	...	1.00	...	0.90	0.98	1.23	0.91
1.101	...	...	1.23	...	1.02	...	...	0.98	...	...

in the red and IR. Asteroid reflectivity curves do not fit into a one-dimensional spectrum of classifications nor is there obvious clustering into well-defined groups. Clusters on plots of *B-V* vs *U-B* (Wood and Kuiper 1963; Chapman *et al.* 1971; Hapke 1971) may be composed of a variety of reflectivities, hence a variety of implied compositions.

Despite the lack of well-defined types, it is useful to attempt an approximate classification. The most distinctive characteristic of the curves is their slope, or over-all "color." Asteroid reflectivities range in slope from quite reddish to nearly flat or slightly bluish. We define three somewhat arbitrary classes of curves—red (R), medium (M), and flat (F). Asteroids in the red slope (R) class constitute half the sample, and most show near-IR absorption bands. Groups are defined within classes by considering absorption band center, location of a UV drop-off, and other characteristics.

Subgroups within the red groups are based on the steepness of the reddish slope (Table III). Strengths of the IR absorption bands in red asteroids seem positively correlated with steepness of slope; this is a reverse of the lunar case in which an admixture of dark reddish glasses not only dominates the spectrum color but reduces multiple scattering among the pyroxene crystals that give rise to the 0.95 μm band (Adams and McCord 1971).

No reddish asteroid shows an absorption band of more than half the strength of Vesta's band. Vesta has an M-type curve and is the only M- or F-type asteroid with a prominent IR band. The asteroids with M-type reflectivities (Table IV) are a small but variegated sample; the data for some are of poorer quality. Some have sharp drop-offs in the UV, while others do not. Some show evidence for a weak band near 0.65 μm.

Asteroids with flat reflectivities comprise a quarter of the sample (Table V). All have quite flat curves throughout the visible and near IR. Some show sharp drop-offs in the near UV, while others clearly do not. None have prominent IR absorption bands.

The center positions of asteroidal absorption bands are tabulated in Table VI along with an indication of our confidence in the reality of the bands. These bands have promising implications for mineralogical identification (Chapman 1972); many are indicative of Fe^{2+} in various pyroxenes and other minerals.

V. PHASE AND ROTATION VARIATIONS OF ASTEROID REFLECTIVITIES

Although measurement of individual asteroids for spectral variations as a function of phase angle or rotation was of secondary concern to our program, there are several useful results.

Ten asteroids were observed during two or more observing runs for which the difference in solar phase angle exceeded 5°. The color variation with phase was calculated from the spectral reflectivity curves in

TABLE III. R-Class asteroids.

Group	Subgroup	Characteristics	Asteroids
R1		Very red. Steep slope 0.3 to 0.85 μm; some leveling beyond 0.85 μm. No prominent band (43 Ariadne may have a deeper band on a different side).	43, 12, 5 (?)
R2		Red asteroids with band near 1.1 μm. Peak near 0.8 μm.	
	R2A	Very red.	39, 7, 5 (?)
	R2B	Moderately red.	68
R3		Red asteroids with 0.95 μm band (band not always statistically certain). Peak near 0.75 μm.	
	R3A	Very red.	192, 79, 40, 82, 5 (?)
	R3B	Moderately red. Weaker band (?)	3, 6, 14
	R3C	Slightly red, weak band.	29
R4		Mostly reddish, curving reflectivities. May have 0.95 μm bands, but statistics low. Probably like Group R3B.	563, 17

approximate *B-V* magnitudes per degree phase angle. It was assumed that there were no confusing variations in color with asteroid rotation. Asteroid 3 (Class R3B) and 192 (R3A) showed probable reddenings with phase of about 0.002 *B-V* mag/deg. Larger but less certain reddenings with phase may have been detected for 7 (R2A) and 40 (R3A). Asteroids 2 (F3) and 704 (F3) seemed to become *bluer* with increasing phase, by 0.01 and 0.02 mag/deg, respectively; such large color changes with phase are unprecedented and should be checked in the future with more complete phase coverage. There were small or doubtful changes in color with phase for asteroids 29 (R3C), 16 (M1), 11 (M4), and 10 (F3). Additionally, for the three asteroids with prominent IR absorption bands (7, 192, and 29) for which we have data, the bands seem deeper at larger phase angles.

These observations suggest a correlation of color-phase effect with asteroid color, which seems physically reasonable, although still requiring observational confirmation. Silicate powders are known to redden with phase, over the range studied here, because the increased pathlength and transmission through grains at larger phase angles enhances their coloration (Adams and Felice 1967). The increase in banddepth with increasing phase angle is also consistent with an enhanced volume component of reflected light at larger phase angles and has been noted for the moon. It is reasonable that materials with less coloration would show a lesser tendency to redden. But a tendency for asteroids with flatter reflectivities to become *bluer* with phase is less easy to understand. It may imply that such asteroids have surfaces composed of opaque grains with preferential red absorption and, hence, blue reflection. Then one might expect an enhancement of the surface component and a bluer coloration with increased phase angle.

TABLE IV. M-Class asteroids.

Group	Characteristics	Asteroids
M1	Slightly red. Flat (no curvature). No band.	16, 11 (??)
M2	Bent curves with dip at 0.65 μm. Steep slope 0.3 to 0.5 μm; flat 0.5 to 0.7 μm; rises again beyond 0.7 μm.	51, 324
M3	Vesta type. Similar to M2 but falls off beyond 0.8 μm. May (4) or may not (409) have deep 0.95 μm band.	4, 409
M4	Fairly flat beyond 0.5 μm. Drops off toward UV below 0.5 μm.	337, 356, 11 (?)

TABLE V. F-Class asteroids.

Group	Characteristics	Asteroids
F1	Like Group M4, except UV downturn is at 0.45 μm.	554, 93 (?)
F2	Bluish. Sharp UV downturn shortwards of 0.4 μm.	13, 1
F3	Flatish or bluish into UV to 0.3 μm.	10, 2, 704
F4	Very bright in UV. Concave upwards.	21

TABLE VI. Band positions in asteroid spectral reflectivities.

Ast. No.	Certainty	Center (μm)		Possible range (μm)	Comments
12	probable		1.10	0.95–>1.10	
	possible	0.64		0.62– 0.73	
39	certain		1.05	0.98–>1.10	deep
	possible	0.64		0.63– 0.67	
7	v. probable		>1.05	1.03–>1.05	deep
43	probable		1.02	0.95–>1.05	
192	certain		0.97	0.92– 1.02	
40	probable		0.94	0.88– 1.00	
79	certain		0.95	0.92– 0.99	fairly sharp
	possible	0.67		0.64– 0.70	
3	certain		0.97	0.93– 1.10	broad, deep
	possible	0.61		0.59– 0.63	
82	v. probable		0.95	0.90– 1.05	seems deep, poor stat.
6	v. probable		0.95	0.91– 1.01	not so deep
	possible	0.67		0.64– 0.69	
68	certain		1.08	1.02–>1.10	deep
17	possible		0.98	0.93– 1.10	poor stat.
14	probable		0.92	0.86– 0.97	poor stat.
	possible	0.65		0.63– 0.67	
29	probable		0.95	0.92– 1.00	not very deep
	possible	0.65		0.63– .067	
563	probable		0.91	0.85– .097	
4	certain		0.95	0.92– 0.98	very deep
324	v. probable	0.66		0.63– 0.69	quite deep, narrow
51	probable	0.69		0.66– 0.75	broad
554	possible	0.66		0.64– 0.75	shallow
409	possible	0.67		0.65– 0.70	
10	possible		1.00	0.95– 1.05	shallow
	probable	0.61		0.58– 0.64	
704	possible	0.64		0.62– 0.66	

However, other studies of asteroid color-phase effects have not yet confirmed the correlation suggested above. Taylor *et al.* (1971) report a reddening with phase for 4 Vesta (M) and 110 Lydia (F). Veverka (1970) found a reddening with phase for all four asteroids he studied, 3 R's and 1 M. The magnitudes of the color-phase effects vary considerably among the asteroids so far measured, although there is no correlation apparent between phase effect and color. Hence the application of standard corrections to all asteroid colors, using the lunar-like phase laws applied by Gehrels (1970) may not be warranted. For this reason, no phase corrections are applied to the reflectivity curves presented in this paper. Fortunately, typical color-phase corrections would not be large enough to change the curve type classification presented in Tables III through V.

Six asteroids showed possible color variations as they rotate. They were observed at least twice during several-day periods too short to expect significant phase effects. In some cases, we know from the rotation period of the asteroid that opposite sides were in fact observed; in other cases the asteroid rotation period is not known. Asteroids suspected of showing color changes with rotation are 6, 10, 16, 43, 68, and 93. Some changes may be due to observational problems, but attempts to confirm rotation effects for these particular asteroids are warranted.

The most significant rotational color change observed is for 6 Hebe. It was observed on three different nights with a maximum equivalent *B-V* color change of at least 0.05 mag, with slope changing through the 0.3 to 0.9 μm range. Although we observed different sides of Hebe, assuming either of two published rotation periods (7.74 or 7.275 hours), we obtained no simultaneous lightcurve so we cannot identify the redder side of Hebe with either lightcurve maximum or minimum.

Taylor and Gehrels (1971 personal communication) have recently reduced some *UBV* data taken on 6 Hebe in 1958/59 and have found a prominent *U-V* rotational color change of about 0.05 mag. These more precise photometric results confirm our cruder measurement. It is significant that Matson (1971b) has reported rotation-correlated changes in thermal flux from Hebe of a factor of 3. Since the epochs of all measurements on Hebe differ, and the pole position is poorly known if at all, it is not yet possible to determine whether all the available data are consistent with a unique model for Hebe. Color variations with rotation have been observed previously for only one other asteroid—Vesta (Bobrovnikoff 1929; Gehrels 1967; Chapman *et al.* 1971).

VI. RELATIONSHIP BETWEEN ASTEROID REFLECTIVITIES AND *UBV* COLORS

Most previous reliable spectrophotometry of asteroids has been done on the *UBV* system and has been summarized by Gehrels (1970). It is therefore of interest to compare our reflectivities with previous *UBV* colors and to derive *UBV*-equivalent colors from our reflectivities for those 16 asteroids not previously studied.

TABLE VII. Approximate *B-V* colors derived from spectral reflectivities (raw data and corrected for color-phase effects).

Ast. Number	Derived Raw	Derived Corrected	Gehrels' (1970) Raw	Gehrels' (1970) Corrected
1	0.64	0.64	0.72	0.71
2	0.63	0.62	0.65	0.65
3	0.82	0.79	0.83	0.81
4	0.74	0.74	0.78	0.77
5	0.83	0.80	0.83	0.82
6	0.86	0.84	0.82	0.82
7	0.81	0.79	0.85	0.83
10	0.71	0.71	0.71	0.70
11	0.78	0.78	0.81	0.80
12	0.87	0.83	...	...
13	0.65	0.64	...	...
14	0.82	0.81	0.82	0.81
16	0.73	0.71	0.71	0.70
17	0.82	0.81	0.85	0.84
21	0.61	0.59	...	...
29	0.76	0.76	0.88	0.87
39	0.91	0.90	0.89	0.88
40	0.82	0.80	0.85	0.83
43	0.97	0.96	...	...
51	0.79	0.78	0.83	0.81
68	0.85	0.84	...	...
79	0.90	0.90	...	...
82	0.90	0.89	...	...
93	0.71	0.69	...	...
192	0.89	0.87	...	...
324	0.81	0.81	...	...
337	0.82	0.82	...	...
356	0.77	0.76	...	...
409	0.73	0.72	...	...
554	0.74	0.75	...	...
563	~0.71	~0.70	...	...
704	0.71	0.70	...	...

We restrict our comparisons to *B-V* colors only due to our calibration problems near the Balmer jump. Our *B-V* equivalent colors do not take account of bandpass differences between the two systems, and therefore the comparisons are only approximate.

Gehrels' *B-V* colors are plotted as *x*'s in Fig. 1 using an assumed *B-V* solar color of 0.63 and scaling to unity at 0.57 μm through a slight extrapolation from the effective wavelength of the *V* filter (0.55 μm). The agreement is excellent, though Gehrels' colors seem slightly redder than ours, despite the small corrections for reddening with phase Gehrels applied to the *UBV* data. The only sizable discrepancies are for 29 Amphitrite and possibly 11 Parthenope, for which Gehrels gives appreciably redder colors.

Table VII lists derived *B-V* equivalent colors for all asteroids observed in our program. Gehrels' results, when available, are shown for comparison along with *B-V* colors *not* corrected for phase (Kuiper *et al.* 1958; Gehrels and Owings 1962). For reasons discussed in Part V above, we see no advantage in using corrected colors, except when the color-phase relation has actually been observed for that particular asteroid, but list both corrected and raw colors for purposes of comparison.

TABLE VIII. Color group criteria.

Source	F	MF	M	MR	R	VR
Spectral reflectivities, this paper, groups	F		M	R2B, R3B, R3C, R4		R1, R2A, R3A
Gehrels (1970), *B-V*	<0.72		0.72–0.80	0.8–0.84		>0.84
Kitamura (1959), C color index	<0.40		0.40–0.51		>0.51	
Fischer (1941), FI color index		<1.0			>1.0	
Sandakova (1955, 1959, 1962), selected, color index		<0.72			>0.72	

VII. COMPREHENSIVE LIST OF ASTEROID COLORS

We desire the largest possible sample of spectral reflectivities in order to test for correlations with orbital and physical parameters which may shed light on asteroid origin, subsequent evolution, and relationship to meteorites. To augment our limited sample, we can use also the more numerous but less descriptive determinations of asteroid "colors." Unfortunately, much early asteroid colorimetry was of poor quality, and recent investigators have wisely restricted their work to the *UBV* data summarized by Gehrels (1970) for 55 asteroids (Chapman *et al.* 1971; Chapman 1971). However, reliable though imprecise colors for additional asteroids were derived in the critical reviews just cited. Combined with the spectral reflectivity results of this paper, they approximately double the number of asteroids with known colors.

Table VIII shows the relationship of the various color indices or classes from the several sources to four adopted color groups: flat (F), medium (M), medium red (MR), and very red (VR). Categories medium flat (MF) and red (R) are used when more precise colors cannot be determined. The final list of colors for 102 asteroids (Table IX) has been derived by giving the greatest weight to *UBV* colors and the spectral reflectivities. Asteroids 60, 127, and 216 are omitted due to conflicting color estimates. It should be recognized that many asteroids with the same colors may have similar but distinctly different reflectivity curve types.

TABLE IX. Reliable colors for 102 asteroids.

1	F*	18	MR*	42	R	89	VR*	341	VR*	532	MR*
2	F*	19	R*	43	VR*	91	MF	345	MF	540	VR*
3	MR*	20	MR*	44	MF	92	M	349	VR	554	F
4	M*	21	F*	45	MF	93	F*	354	VR*	563	MR*
5	VR*	22	F*	51	M*	95	MF	356	M*	624	M
6	MR*	23	VR*	52	MF*	110	F*	372	MF	658	VR*
7	R*	25	VR*	57	R	115	R*	380	F*	674	R
8	VR*	27	MF*	61	VR*	122	F*	385	R	675	R
9	VR*	29	R*	62	M*	124	R	402	R	704	F*
10	F*	30	VR*	64	MF	179	R	409	M	779	MF
11	M*	31	MF	68	MR*	182	R	433	VR*	911	M*
12	VR*	32	R	69	MF	192	VR*	478	M	976	M*
13	F*	34	F	70	MF	258	R	481	R	1043	VR*
14	MR*	37	VR*	77	R*	268	F*	485	M	1287	VR*
15	M*	38	M	78	F*	321	MR*	498	M*	1291	MR*
16	MF*	39	VR*	79	VR*	324	M*	510	M*	1437	F*
17	R*	40	R*	82	VR*	337	M*	511	F	1620	MR*

* Indicates particularly reliable colors.

VIII. CORRELATION OF COLORS WITH ORBITAL PARAMETERS

For those asteroids away from planets and commensurabilities, it is generally believed that the distribution of orbits resembles that at the time asteroids were formed. Any correlation of asteroid colors (hence compositions) with semimajor axis a or with orbital Jacobi constant could indicate differences in the condensation of the solar nebula as a function of heliocentric distance. Correlations of color with inclination might reflect analogous early compositional variation perpendicular to the ecliptic.

Discontinuities in color with increasing perihelia might reveal the boundary of the ice stability field in the solar system (cf. Watson *et al.* 1963). Color correlations with inclination or eccentricity might clarify microparticle erosional processes as a function of mean impact velocity since high-velocity shock and vitrification affect surface colors.

In order to examine such possible correlations, we used two sets of asteroid proper elements: (1) those provided by J. Arnold (see Arnold 1969) for the entire sample of 102 asteroids, and (2) recently redetermined elements provided by Williams (see Williams 1971) for our sample of 32 asteroids with determined spectral reflectivities. Williams took into account higher terms in the expansions for both e and i and considered both free and forced oscillations. The two sets are sufficiently similar for the purposes considered here.

A. Correlation of Color with a, e, and i

Several earlier investigators reported correlations between asteroid colors and a or the invariant Jacobi constant with respect to perturbations by Jupiter (a function of a, e, and i), especially correlations with extreme values of a.

Figure 2 shows 102 asteroid colors plotted as a function of a and e. Triangles are reds, circles are F's and M's. There is a clear but imperfect correlation of color with a. For $a<2.6$ AU there are 12 MF asteroids and 28 R ones, while for $a>2.6$ AU there are 37 MF's

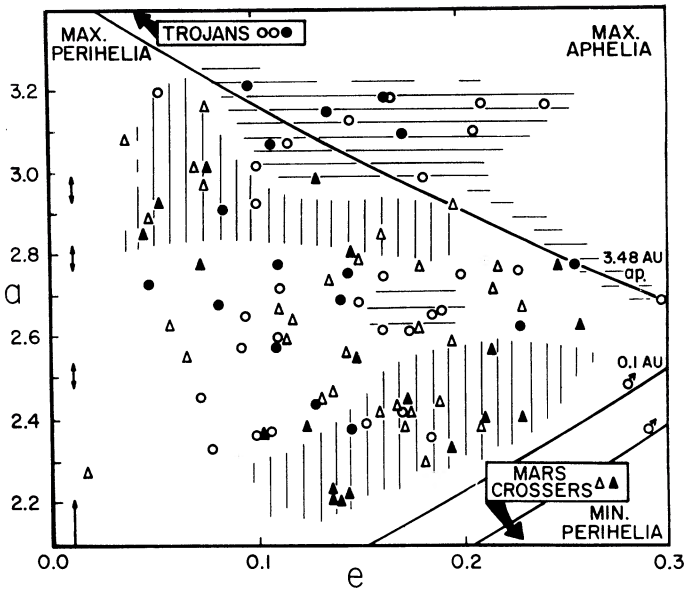

FIG. 2. Asteroid colors (triangle = red, circle = medium or flat reflectivities) are plotted as a function of asteroid semimajor axis (a) and proper eccentricity (e). *Filled-in symbols* indicate more extreme reflectivities (red or flat). Three asteroids at large a ("Trojans") and two at small a ("Mars crossers") plot off the field of the graph, but their colors are shown in the boxes. *Three lines* drawn across the graph represent the locus of points corresponding to an aphelion distance of 3.48 AU, and perihelion distances approaching Mars within 0.1 and 0.0 AU. The *arrows* along the left axis indicate positions of the major Kirkwood gaps. *Vertical cross-hatchings* indicate regions where reddish colors predominate and *horizontal cross-hatchings* where MF colors predominate. Unhatched regions indicate more equally distributed colors or regions for which there is insufficient data to specify the predominate colors.

and 25 R's. The correlation exists even excluding Trojan and Mars asteroids, but it is clearly strongest at extreme values of a. The shadings in Fig. 2 show regions where either the MF's or the R's tend to predominate. A prominent feature is the sharp cutoff for red colors at an aphelion distance of about 3.5 AU. This would be consistent with a model in which a solar nebula condensate with flat spectral reflectivity was restricted by pressure–temperature relations to the outer regions of the asteroid belt and was a late component to accrete (perhaps carbonaceous chondritic matter; cf. Larimer and Anders 1967).

Also, Fig. 2 shows a tendency for asteroids with minimal perihelia to be reddish; few asteroids with flat reflectivities have perihelia within 2 AU. This correlation may reflect processes of formation or of subsequent evolution which are governed by maximum temperatures reached, rather than by mean temperature, such as escape of volatiles. (But there is no obvious color difference correlated with larger perihelion distances, so any ice-stability field is not readily recognizable in asteroid colors.) If most meteorites are fragments of Mars-crossing, or nearly Mars-crossing asteroids (Anders 1971), the preponderance of reddish asteroids with perihelia closer to Mars than 0.2 AU indicates that meteorite collections may be biased towards reddish compositions. Asteroid 324 Bamberga is the exception to this rule, but it also reaches a large aphelion distance.

There seems to be no simple correlation between asteroid color and either e or i. This is true even for extreme values. Whatever correlation there is between color and Jacobi constant seems due solely to the correlation with a.

The Kirkwood gaps are shown by arrows in the left portion of Fig. 2. A tendency for asteroids near the borders of the gaps to be red is shown in Table X, but requires confirmation.

Of the sample of 32 asteroids with measured spectral reflectivities, there is a suggestion that those with prominent absorption bands are restricted to small and intermediate values of a, with a possible clustering of those containing the 0.95 μm band near $a = 2.55$ (± 0.2), $e = 0.2$ (± 0.5). Williams has listed for us the minimum distance of approach to Mars for the 32 asteroids; of 12 with a minimum distance less than 0.2 AU, 8 are class R, 2 M, and 2 F, and of 6 that approach Mars within 0.08 AU, 5 are R, 1 M. There may be a tendency for asteroids with bright UV reflectivities to be in the center and towards the upper right of a plot such as that of Fig. 2, while those with sharp UV drop-offs in their reflectivity curves are in the center and toward the lower left. There is no correlation between curve type and i. Since curve types chiefly reflect mineralogical composition (Chapman 1972), theories for chemical origin of asteroids may be tested by such correlations once more reflectivity curves are available.

B. Colors and Hirayama Families

The Hirayama families of asteroids are usually thought to be composed of fragments from catastrophic collisions. Clearly, the colors of collisional fragments from a body of uniform composition should appear

TABLE X. Asteroid colors by distance from edges of Kirkwood gaps.

	No. MF	No. R	Percentage MF
Within Kirkwood gaps	4	12	25%
0.0 to 0.05 AU from edge	13	19	41%
0.05 to 0.1 AU from edge	20	17	54%
Beyond 0.1 AU from edge	9	3	75%

TABLE XI. Correlation of color with lightcurve amplitude.

Max. amplitude (magnitudes)	F	MF and M	MR and R	VR
<0.2	5	6	4	5
>0.2	5	5	9	10

identical. Depending upon the fragmentation process, fragments of a mineralogically differentiated body probably would differ in color. (Since most catastrophic collisions are between a large asteroid and one much smaller, rather than between similar-sized objects, one expects most or all of the larger fragments to be from the large asteroid only.) Recent work by Alfvén and Arrhenius (1970) and others raises the possibility that dynamical focusing mechanisms may bring previously unrelated asteroids together into families. Presumably such asteroids would show a variety of colors.

There is no certainty that a particular asteroid is a member of a family; there is a chance that it is a "field" asteroid. Although Williams (private communication 1971) largely confirms the existence of the *families* reported by Arnold (1969), his analysis considerably modifies the assignment of *individual asteroids* to those families. In the search for correlations of color with family membership, we give preference to Williams' data when it is available.

Asteroids 17 (color group R4 or R3B) and 79 (R3A), listed by Arnold as members of family B-25, may be family members according to Williams. Due to our large error bars for 17 Thetis, the two asteroids are identical to within errors.

Williams lists 1 Ceres (F2), 39 Laetitia (R2A), and 93 Minerva (F1) as family members. The uncertainty in the color for Minerva is sufficiently large that it can hardly be distinguished from Ceres, but Laetitia is obviously very different.

The Flora group is a large family with several recognizable subdivisions. Williams regards 43 Ariadne (R1=VR) to be a member of the Flora family. 8 Flora is also VR in color. Arnold regards asteroid 341 (VR) to be in the same subgroup, and asteroid 540 (also VR) to be in the next subgroup. Thus all Flora members with known colors seem very red, which is noteworthy since many are known Mars crossers and this family is a likely source for meteorites.

Both Arnold and Williams agree that 19 Fortuna (R) and 21 Lutetia (F4) are members of family A-82. They clearly differ in color. Colors are known (Table IX) for pairs from six additional families as listed by Arnold; the members of three pairs seem clearly different in color while the remaining three could be similar in color. Asteroids 12 (R1=VR), 115 (R), and 192 (R3A=VR), all members of possible jet stream J-2, are similar in color but the details of the reflectivities of 12 Victoria and 192 Nausikaa clearly differ.

In summary, there is no uniformity of color within most asteroid families. Hence most families are not composed of fragments of homogeneous bodies.

IX. CORRELATION OF COLOR WITH PHYSICAL PROPERTIES OF ASTEROIDS

Any correlations between asteroid spectral reflectivity and such physical characteristics as diameter may have important implications for understanding the origin of asteroids. For instance, Mason's (1968) model for the development of meteorite parent bodies implies a relationship between parent body size and meteorite type. Mason derives achondrites from asteroids sufficiently large to have differentiated and chrondites from smaller bodies. These two meteorite classes indeed have distinct spectral reflectivities which are represented in the asteroid belt (Chapman 1972).

The number of asteroids for which physical properties have been determined is small. Hence attempts to correlate asteroid color with physical properties are compromised by small sample size.

The obliquities of asteroid rotation axes are very poorly known (Vesely 1971), but there are more than 40 asteroids with known colors for which lightcurves have been measured (Gehrels 1970; Yang *et al.* 1965). We find no obvious correlation between color and rotation period.

There may be a weak correlation between color and lightcurve amplitude; see Table XI. We adopt the maximum amplitude so far observed, but recognize that these are lower limits because some asteroids may have been observed approximately pole-on. Asteroids showing large amplitudes are predominantly red in color. This may reflect the stronger correlation we find below between color and size, provided smaller asteroids have larger lightcurve amplitudes. That they do is not yet proven, but is consistent with fragmentation histories developed by Anders (1965) and observations by van Houten (Gehrels 1970, p. 326).

A. Correlation of Color with Absolute Magnitude $B(1,0)$

We first address the fundamental question of correlation of asteroid color with size from the classic viewpoint that asteroid absolute magnitudes can be converted into relative sizes. We know from the polarization studies of Veverka (1970) and the thermal infrared measurements of Matson (1971a, b) and Allen (1971), that there is a large scatter among asteroidal albedos—at least a factor of 10. Table XII shows the

TABLE XII. Correlation of asteroid color with absolute magnitude $B(1,0)$.

	Spectral reflectivity			
$B(1,0)$	Very red	Medium red	Medium	Flat
<6.0	0	0	1	2
6.0–8.5	10	12	9	5
8.5–11.0	7	14	21	10
>11.0	6	3	1	0

correlation of asteroid color with $B(1,0)$, grouped in magnitude intervals of 2.5 which smear out differences due to albedo and assure a relative diameter grouping. The table shows that the three largest asteroids (Ceres, Pallas, Vesta) have flat reflectivities, while the 10 smallest asteroids are predominantly red. Therefore, there is a correlation between color and the extremes of the asteroid size distribution.

B. Correlation of Color with Diameter

We can test for a color–diameter correlation more directly using the small sample of asteroids for which diameters have recently been determined by Matson (1971b) and others. We present two samples of data in Table XIII. In Table XIII-A, we show the relationship between color and diameter using those asteroids plotted on Matson's Figs. 33 and 34, representing his best results. Shown in Table XIII-B is the same relationship for a larger sample which includes as well some asteroids less well observed by Matson (from his Figs. 12–14) and those studied by Veverka (1970). In both cases, the correlation between reddish reflectivities and small size is quite strong. No large asteroids are red, no small ones clearly have flat reflectivities. The demarcation is near 250±50 km diam. The result is consistent with the correlation found between color and $B(1,0)$ and has important implications.

It should be emphasized that the color correlation is not a simple one in that several reflectivity curve types are included in each color category. For instance, Ceres and Pallas both fall in the F category despite the fact their reflectivities differ substantially in the UV. However, it is plausible that several types of flattish reflectivities all indicate a composition expected for the surfaces of chemically differentiated asteroids while the reddish reflectivities indicate undifferentiated compositions. It is premature to assert proof from these correlations that asteroids larger than 250 km diam are differentiated, but further study along these lines is clearly warranted. Note also that Hartmann (1968) has predicted that 250±100 km is the demarcation between original accretions and fragments. A more detailed dicussion of the implications of this correlation, invoking mineralogical determinations for asteroid surface compositions will appear in Chapman (1972).

C. Correlation of Color with Albedo

Using the same data from Matson (1971b) and Veverka (1970) described above, we have determined a relative sequence of asteroid albedos. There is no prominent correlation between color and albedo for the relatively small sample available. There are examples of high-albedo asteroids which have both reddish reflectivities (e.g., 39 Laetitia) and flatter ones (4 Vesta) while low-albedo asteroids have reflectivities ranging from reddish (7 Iris) to medium (324 Bamberga). However, since both color and albedo are determined by composition, one might expect partial correlation, probably in the sense of low albedo being correlated with flat reflectivities. If color and albedo were correlated, then the color–diameter correlation described above would imply a correlation between albedo and diameter. This might render invalid earlier studies of the size–frequency distribution for asteroids based on assumptions of constant albedo (Chapman 1971). Therefore, it is important to search further for such correlations from a larger asteroid sample, taking due account of selection biases inherent in the albedo measurements.

APPENDIX: ABSOLUTE CALIBRATION OF SOLAR SYSTEM SPECTRAL REFLECTIVITIES

A series of papers has been published by the M.I.T. Planetary Astronomy Laboratory on solar system spectral reflectivities (see footnote to Table A.2). We use a new set of absolute calibrations in this paper for the first time and compare it with our previous calibrations in this Appendix. The study of these calibrations is a continuing process which gradually converges toward the best calibrations possible. Those discussed here are an intermediate step and subsequently will be replaced by still better ones on which work has been completed (Elias 1972).

Previous reductions of this Laboratory used: (1) the same Oke (1964) star calibrations; (2) an observationally determined absolute spectrum of Alpha Lyrae (Oke and Schild 1970); (3) the solar spectrum of Labs and Neckel (1968); (4) an assumed square-wave response for our filters; and (5) no consideration of the small effective-wavelength shifts due to spectral responses of the photomultipliers, mirrors, or atmosphere.

The model spectrum of Alpha Lyrae (Vega) used here agrees well with the earlier spectrum in gross character but also takes account of stellar lines. The new solar spectrum of Arvesen *et al.* (1969), obtained at 12 km altitude in a NASA jet, has an estimated

TABLE XIII. Correlation of asteroid color with size.

A. Small sample: well-established diameters

Diameter	Spectral reflectivity VR	MR	M	F
Small	2	3	2	0
Medium	0	1	1	0
Large	0	2	1	0
Very large	0	0	1	2

B. Larger sample: approximate diameters

Diameter	Spectral reflectivity VR	MR	M	F
Small	6	4	2	0
Medium	1	2	2	0
Large	0	2	1	0
Very large	0	0	1	2

accuracy of 1%, while the spectrum of Labs and Neckel, obtained at the Jungfraujoch, is 5% low shortwards of 0.5 μm. The resolution of the new spectrum is better and the tabulation convenient for digitization so that solar lines can be taken into account accurately.

We have calculated Vega/Sun ratios at well-defined effective wavelengths for each filter determined from their spectral responses, taking into account the instrument spectral response. To calculate the star/Sun ratios in Table A.1 [the final two terms of Eq. (1)], we have interpolated into the Oke and Hayes star calibrations at these effective wavelengths. Changes in the effective wavelengths by atmospheric absorptions yield star/Sun ratio corrections of the order of 1% or less for all filters except Nos. 1 and 2.

The chief source of uncertainty seems to be in the Oke and Hayes star calibrations relative to Alpha Lyrae. These errors (chiefly scatter but some slope error) have been estimated by Breger (1971) as follows:

Wavelength (μm):	0.3–0.4	0.4–0.5	0.5–0.6	0.6–0.9	0.9–1.1
Error:	3%	1%	2%	3%	4%

TABLE A-1. Star/Sun ratios.

Filter	ξ^2 Cet	ϵ Ori	γ Gem	η Hya	α Leo	θ Crt
1	4.1091	16.9409	2.9566	13.5018	6.5361	4.7573
2	3.0589	12.0292	2.2577	9.3936	4.7492	3.4845
3	2.3733	8.7788	1.7857	6.5875	3.5739	2.6176
4	2.1826	7.4397	1.7309	5.5840	3.1560	2.4153
5	3.1819	6.0479	2.6119	4.2062	3.8260	3.0509
6	2.8168	3.1652	2.7368	3.2381	2.9860	2.8942
7	2.1028	2.2671	2.0804	2.3450	2.2112	2.1567
8	1.5450	1.6316	1.5600	1.6940	1.6043	1.5934
9	1.2952	1.3463	1.3134	1.3780	1.3402	1.3387
10	1.1723	1.1918	1.1798	1.2137	1.1876	1.1911
11	1.0000	1.0000	1.0000	1.0000	1.0000	1.0000
12	0.8581	0.8527	0.8764	0.8537	0.8666	0.8719
13	0.7705	0.7523	0.7857	0.7423	0.7673	0.7635
14	0.6766	0.6551	0.6869	0.6330	0.6719	0.6584
15	0.6412	0.6186	0.6589	0.5961	0.6403	0.6295
16	0.6073	0.5837	0.6365	0.5628	0.6064	0.6025
17	0.5703	0.5401	0.6040	0.5229	0.5629	0.5649
18	0.5301	0.5020	0.5643	0.4779	0.5265	0.5255
19	0.5249	0.4716	0.5700	0.4545	0.5165	0.5229
20	0.5069	0.4188	0.5581	0.4184	0.4987	0.5032
21	0.4672	0.3730	0.5214	0.3786	0.4597	0.4673
22	0.4522	0.3554	0.5253	0.3525	0.4242	0.4439
23	0.4235	0.3306	0.4858	0.3221	0.3933	0.3988
24	0.3930	0.3069	...	...	0.3605	...

Filter	θ Vir	109 Vir	ζ Oph	ϵ Aqr	29 Pis	η Pis
1	3.1123	3.3166	11.3804	2.8594	8.2523	...
2	2.3730	2.5119	8.2044	2.1889	5.9600	...
3	1.8767	1.9898	6.1108	1.7557	4.4496	...
4	1.7974	1.8770	5.3404	1.6883	3.9207	...
5	2.6705	3.0250	4.5017	2.8915	4.2664	...
6	2.7099	2.7249	2.4902	2.6960	3.0879	0.5958
7	2.0534	2.0481	1.8682	2.0388	2.2433	0.7100
8	1.5340	1.5114	1.4128	1.5036	1.6226	0.8227
9	1.2974	1.2985	1.2332	1.2876	1.3389	0.8557
10	1.1646	1.1666	1.1534	1.1621	1.1858	0.9712
11	1.0000	1.0000	1.0000	1.0000	1.0000	1.0000
12	0.8764	0.8723	0.8775	0.8750	0.8582	0.9988
13	0.7759	0.7845	0.8043	0.7821	0.7585	1.0629
14	0.6772	0.6928	0.7162	0.6897	0.6607	1.0524
15	0.6527	0.6626	0.6992	0.6670	0.6308	1.1220
16	0.6269	0.6323	0.6746	0.6411	0.5995	1.1518
17	0.5915	0.5970	0.6389	0.6073	0.5601	1.1614
18	0.5569	0.5654	0.6089	0.5681	0.5207	1.1709
19	0.5578	0.5651	0.5854	0.5678	0.5103	1.2225
20	0.5432	0.5556	0.5310	0.5594	0.4800	1.2465
21	0.5106	0.5121	0.4811	0.5178	0.4348	1.1992
22	0.4975	0.5003	0.4647	0.5073	0.4162	1.2245
23	0.4489	0.4729	0.4392	0.4820	0.4403	1.2313
24	...	0.4389	0.4078	0.4588	0.3856	1.2319

Breger regards ξ^2 Ceti as the best secondary standard in the sky, which is the star we used most often. The interpolation between bandpasses measured by Oke and Hayes is somewhat uncertain; they avoided stellar lines which our filters do not necessarily do so. Such effects are small except for filter 5 which straddles the Balmer jump and for which errors are in the 5% to 10% range.

These calibrations are at least as sound as the more commonly used calibrations against G-type stars with "solar" spectra, though there is a remote possibility of unknown systematic error. However, we believe the errors in our calibrations are well known, while to the best of our knowledge there has been no definitive analysis of the assumptions and errors inherent in calibrations against G-type stars.

We found previously that diverse solar system objects reduced with the earlier calibrations showed identical "unnatural" characteristics, suggesting imperfect standardization. When laboratory reflectivities of Apollo 11 soil samples (Adams and Jones 1970) were compared with telescopic reflectivities of the 15-km spot centered on the landing site, it was found that some structure in the telescopic data was not evident in the soil, despite an over-all similarity in shape (McCord and Johnson 1970). Therefore, approximate "smoothing factors" were devised to remove from the telescope data major features in solar system spectra not confirmed by the "ground truth" soil measurements. These factors (see Table A.2) have been applied generally to our reflectivities during the past year on the assumption that they correct for plausible calibration errors. This procedure is valid provided that the lunar soil is homogeneous on a scale of kilometers so that the submillimeter size fraction of soil returned from one or a few lunar localities is representative. There are reasons for doubt, including the presence of kilometer-scale color boundaries in the maria indicating little lateral mixing and evidence that the compositions of lunar soil particles are strongly

TABLE A-2. Smoothing factors and new calibrations.[a]

Filter	Smoothing factor: Lunar	Smoothing factor: Nonlunar	New calibration factor
1	0.6486	0.9728	0.8
2	0.8248	0.9728	0.884
3	0.9622	0.9728	0.909
4	1.0589	0.9728	1.023
5	1.1664	0.9728	1.048
6	0.9609	0.9728	0.911
7	0.9728		0.915
8	0.9728		0.969
9	0.9728		0.955
10	1.0170		0.985
11	1.0000		1.000
12	1.0130		0.984
13	1.0210		0.976
14	0.9689		0.970
15	0.9796		1.000
16	0.9728		1.013
17	0.9767		1.017
18	0.9728		1.028
19	0.9698		1.029
20	0.9728		1.002
21	0.9728		0.954
22	0.9728		0.968
23	0.9728		0.945
24	0.9728		0.955

[a] Prior to the present paper, there have been three different calibrations used: (I) Early unsmoothed data are given in Adams and McCord (1970), Johnson and McCord (1970), McCord and Johnson (1970), McCord *et al.*, (1970), and Johnson (1971). (II) Smoothing factors were used for the following nonlunar papers; Lebofsky *et al.*, (1970), Pilcher and McCord (1971), McCord and Westphal (1971), Johnson *et al.*, (1971), McCord *et al.*, (1971a), McCord *et al.*, (1971b), Chapman *et al.*, (1971), Johnson and McCord (1971), and McCord and Adams (1972). (III) Different smoothing factors were used for filters 1–6 for the following lunar papers: Adams and McCord (1971), McCord *et al.*, (1972a), and McCord *et al.* (1972b). To convert reflectivities in (I) to the new calibration, multiply by the nonlunar smoothing factor *and* the new calibration factor. For (II), multiply by the new calibration factor alone. For (III), multiply as for (I) but then divide by the lunar smoothing factor. Several earlier papers contain some data taken with an earlier Caltech filter set; they may be converted (but only approximately) to the new calibration by interpolating in this table to the appropriate wavelength (see Table I).

size-dependent (LSPET 1971). Studies of Apollo 14 and 15 soils (but Apollo 12 is questionable) seem to have largely confirmed the approach and resulting smoothing factors to the old calibrations obtained from Apollo 11.

Because of the improvements in the direct stellar and solar calibrations and uncertainties in the lunar soil calibration, we adopt the new calibrations with no smoothing factors for this paper. We have examined the ensemble of reflectivities for asteroids and other solar system objects reduced with the new calibrations and find no convincing evidence for substantial systematic departures from "normal" reflectivity curves for those diverse bodies to indicate the need for calibration corrections. The analysis of Elias (1972) will be the next step in our study of these problems.

ACKNOWLEDGMENTS

This article is a condensation and revision of Chaps. III–VI and Appendix V of the senior author's doctoral dissertation at M.I.T. He wishes to thank the numerous individuals who are acknowledged therein. Dr. T. Gehrels and Dr. E. Anders provided helpful critiques of those chapters. J. Elias, of the M.I.T. Planetary Astronomy Laboratory, is largely responsible for calculating the stellar calibrations discussed in the Appendix. L. Lebofsky spent many nights assisting us in the observations. P. Herget provided asteroid ephemerides, J. Arnold sent us a card deck of orbital elements, and D. Matson and J. Williams provided data prior to publication. The authors were Guest Investigators at the Hale Observatories on several occasions. We also used the facilities of the Division of Geological Sciences at Caltech (through the courtesy of J. Westphal) and of the Kitt Peak National Observatory. Partial financial support was provided by NASA grants NGR-22-009-473 and NGR-22-009-583. Some work on preparing this article for publication was done while the senior author was in residence at IIT Research Institute.

REFERENCES

Adams, J. B., and Felice, A. L. (1967). J. Geophys. Res. **72,** 5705.
Adams, J. B., and Jones, R. L. (1970). Science **167,** 737.
Adams, J. B., and McCord, T. B. (1970). Geochim. Cosmochim. Acta **3,** 1937.
Adams, J. B., and McCord, T. B. (1971). Science **171,** 567.
Alfvén, H., and Arrhenius, G. (1970). Astrophys. Space Sci. **8,** 338 (1970); Astrophys. Space Sci. **9,** 3.
Allen, D. A. (1971). In *Physical Studies of Minor Planets*, edited by T. Gehrels, NASA SP-267 (1).
Anders, E. (1965). Icarus **4,** 399.
Anders, E. (1971). In *Physical Studies of Minor Planets,* edited by T. Gehrels, NASA SP-267 (1971), p. 429.
Arnold, J. R. (1969). Astron. J. **74,** 1235.
Arvesen, J. C., Griffin, R. N., and Pearson, B. D., Jr. (1969). Appl. Opt. **8,** 2215.
Bobrovnikoff, N. T. (1929). Lick Obs. Bull. **18,** 18.
Breger, M. (1971). SUNY Stony Brook Comm. in Astron. (1).
Chapman, C. R. (1971). "Surface Properties of Asteroids," doctoral dissertation, Massachusetts Institute of Technology.
Chapman, C. R. (1972). In preparation.
Chapman, C. R., Johnson, T. V., and McCord, T. B. (1971). In *Physical Studies of Minor Planets*, edited by T. Gehrels, NASA SP-267 (1971), p. 51.
Elias, J. (1972). Master's dissertation, Massachusetts Institute of Technology.
Fischer, V. H. (1941). Astron. Nachr. **272,** 127.
Gehrels. T. (1967). Astron. J. **72,** 929.
Gehrels, T. (1970). In *Surfaces and Interiors of Planets and Satellites,* edited by A. Dollfus (Pergamon Press. London, 1970), p. 317.
Gehrels, T., and Owings, D. (1962). Astrophys. J. **135,** 906.
Hapke, B. (1971). In *Physical Studies of Minor Planets*, edited by T. Gehrels, NASA SP-267, p. 67.
Hartmann, W. K. (1968). Astrophys. J. **152,** 337.
Hayes, D. S. (1970). Astrophys. J. **159,** 165.
Johnson, T. V. (1971). Icarus **14,** 94.
Johnson, T. V., Lebofsky, L. A., and McCord, T. B. Publ. Astron. Soc. Pac. **83,** 93.
Johnson, T. V. and McCord, T. B. (1970). Icarus **13,** 37.
Johnson, T. V., and McCord, T. B. (1971). Astrophys. J. **169,** 589.
Kitamura, M. (1959). Publ. Astron. Soc. Pac. **11,** 79.

Kuiper, G. P., Fujita, Y., Gehrels, T., Groeneveld, L., Kent. J., Van Biesbroeck, G., and Van Houten, C. J. (1958). Astrophys. J. Suppl. Ser. **3,** 289 .
Labs, D., and Neckel, H. (1968). Z. Astrophys. **69,** 1 .
Larimer, J. W. and Anders, E. (1967). Geochim. Cosmochim. Acta **31,** 1239 .
Lebofsky, L. A., Johnson, T. V., and McCord, T. B. (1970). Icarus **13,** 226 .
LSPET (Lunar Sample Preliminary Examination Team) (1971). Science **173,** 681 .
Mason, B. (1968). In *Extraterrestrial Matter*, edited by C. A. Randall, Jr. (Northern Illinois Univ. Press, De Kalb, Illinois, 1968), pp. 3–22.
Matson, D. L. (1971a). In *Physical Studies of Minor Planets,* edited by T. Gehrels, NASA SP-267, p. 45.
Matson, D. L. (1971b). "Infrared Emission from Asteroids at Wavelengths of 8.5, 10.5, and 11.6 μm," doctoral dissertation, Calif. Inst. of Technology .
McCord, T. B. (1968). Appl. Opt. **7,** 475 .
McCord, T. B., and Adams, J. B. (1972). Science **178,** 745 .
McCord, T. B., Adams, J. B., and Johnson, T. V. (1970). Science **168,** 1445 .
McCord, T. B., Charette, M., Johnson, T. V., Lebofsky, L. A., and Pieters, C. (1972a). J. Geophys. Res. **77,** 1349 .
McCord, T. B., Charette, M., Johnson, T. V., Lebofsky, L. A., and Pieters, C. (1972b). The Moon **5,** 52.
McCord, T. B., Elias, J., and Westphal, J. A. (1971a). Icarus **14,** 245 .
McCord, T. B., and Johnson, T. V. (1970). Science **169,** 855 .
McCord, T. B., Johnson, T. V., and Elias, J. (1971b). Astrophys. J. **165,** 413 .
McCord, T. B., and Westphal, J. A. (1971). Astrophys. J. **168,** 141 .
Oke, J. B. (1964). Astrophys. J. **140,** 689 .
Oke, J. B., and Schild, R. E. (1970). Astrophys. J. **161,** 1015 .
Pilcher, C. B., and McCord, T. B. (1971). Astrophys. J. **165,** 195 .
Sandakova, E. V. (1955). Astron. Circ. USSR (163).
Sandakova, E. V. (1959). Publ. Kiev Univ. Astron. Obs. (8).
Sandakova, E. V. (1962). Publ. Kiev Univ. Astron. Obs. (10).
Schild, R. E., Peterson, E. M., and Oke, J. B. (1971). Astrophys. J. **166,** 95 .
Taylor, R. C. (1971). In *Physical Studies of Minor Planets*, edited by T. Gehrels, NASA SP-267, p. 117.
Taylor, R. C., Gehrels, T., and Silvester, A. B. (1971). Astron. J. **76,** 141 .
Veverka, J. F. (1970). "Photometric Studies of Minor Planets and Satellites," doctoral dissertation, Harvard University .
Vesely, C. D. (1971). In *Physical Studies of Minor Planets*, edited by T. Gehrels, NASA SP-267 (1971), p. 133.
Watson, K., Murray, B. C., and Brown, H. (1963). Icarus **1,** 317 .
Williams, J. G. (1971). In *Physical Studies of Minor Planets,* edited by T. Gehrels, NASA SP-267 (1971), p. 177.
Wood, H. J. and Kuiper, G. P. (1963). Astrophys. J. **137,** 1279 .
Yang, X., Zhang, Y., and Li, X. (1965). Acta Astronomica Sinica **13,** 66 .

*Contribution No. 55 of the M.I.T. Planetary Astronomy Laboratory.

†All three authors were visiting astronomers, Kitt Peak National Observatory, which is operated by the Association of Universities for Research in Astronomy, Inc., under contract with the National Science Foundation.

‡Presently at Planetary Science Institute, 252 West Ina Road, Tucson, Arizona 85704.

§Presently at Jet Propulsion Laboratory, 4800 Oak Grove Drive, Pasadena, California 91103.